

## Temperature Dependence of Spin-Transfer-Induced Switching of Nanomagnets

I. N. Krivorotov, N. C. Emley, A. G. F. Garcia, J. C. Sankey, S. I. Kiselev, D. C. Ralph, and R. A. Buhrman

Cornell University, Ithaca, New York, 14853 USA  
(Received 19 March 2004; published 15 October 2004)

We measure the temperature, magnetic-field, and current dependence for the switching of nanomagnets by a spin-polarized current. Depending on current bias, switching can occur between either two static magnetic states or a static state and a current-driven precessional mode. In both cases, the switching is thermally activated and governed by the sample temperature, not a higher effective magnetic temperature. The activation barriers for switching between static states depend linearly on current, with a weaker dependence for dynamic to static switching.

DOI: 10.1103/PhysRevLett.93.166603

PACS numbers: 72.25.Ba, 75.20.-g, 75.75.+a

The interaction between the magnetic moment of a metallic ferromagnet and a spin-polarized electrical current results in the spin-transfer effect [1–8], whereby the current can apply a torque to the magnet via transfer of angular momentum. The manipulation of nanomagnets by spin-transfer torques is under investigation for use in the switching of nonvolatile memory elements [9] and for current-tunable microwave sources [10,11]. Previous measurements of magnetic switching driven by spin-polarized currents have suggested that the process is thermally activated [12–14], but there remains disagreement about the switching mechanism. One set of models describes the effect of a spin-polarized current in terms of a torque that coherently rotates the local moment of the magnet, as described within the framework of the Landau-Lifshitz-Gilbert (LLG) equation [1,15–17]. An alternative model proposes that when the polarization of the current is opposite to the moment of the magnet, spin-flip scattering of electrons excites incoherent nonuniform magnons, effectively raising the magnetic temperature so as to accelerate switching [13,14]. In this Letter, we use measurements of the switching rates as a function of temperature, magnetic field, and current to distinguish between these mechanisms. We find that a single sample can undergo different switching processes between separate static and dynamic states, that were not all distinguished in previous studies. In all cases, switching is thermally activated and governed by the actual background sample temperature. We observe no magnetic-configuration-dependent heating. The data are described well by current-dependent activation barriers that agree with predictions of the LLG-based models.

The samples we study are made from Cu(100 nm)/Py( $X$  nm)/Cu(6 nm)/Py(2 nm)/Cu( $Y$  nm)/Pt(30 nm) multilayers deposited by magnetron sputtering, where  $X = 12$  or 20 nm for the thicker permalloy (Py = Ni<sub>80</sub>Fe<sub>20</sub>) layer and  $Y = 2$  or 20 nm. Electron-beam lithography and ion milling are used to define an elliptical pillar structure with a size  $130 \times 60$  nm and with both magnetic layers etched through [5,18]. We will analyze the switching properties of the two-nanometer thick Py “free layer”.

Positive currents are defined so that electrons flow from the thinner to thicker Py layer. Although we focus below on one Py(20 nm)/Cu(6 nm)/Py(2 nm) device, similar results were obtained in eight samples.

Figure 1(a) displays the differential resistance ( $dV/dI$ ) versus magnetic field ( $H$ ) applied in plane along the major axis of the nanopillar, at the temperature  $T = 295$  K. The field drives the free-layer moment between a low-resistance orientation parallel (P) to the fixed Py layer and a higher-resistance antiparallel (AP) state. The transition is continuous and reversible at 295 K and hysteretic at 4.2 K [Fig. 1(b)], indicating that the free layer is superparamagnetic at 295 K. The dipolar field from the fixed Py layer ( $H_d$ ) causes the midpoint of the hysteresis loop to be shifted from  $H = 0$ . Figs. 1(c) and 1(d) show that the orientation of the free-layer moment can be controlled by the current ( $I$ ) as well as  $H$ . At 4.2 K the current hysteresis loop is not square, unlike the field loop. Starting in the low-resistance P state, as  $I$  is increased there is a continuous increase in  $dV/dI$  at  $I_D^+$  prior to the abrupt switching to the AP state at  $I_S^+$  [10,13]. From

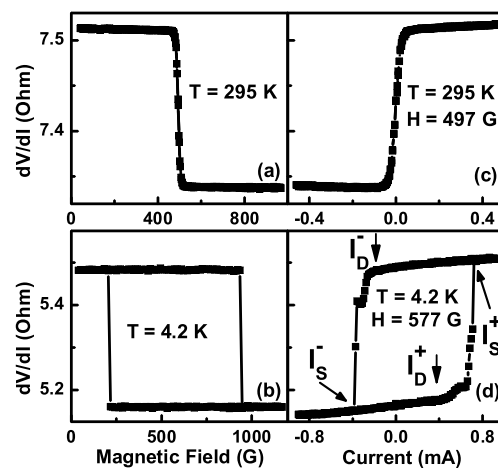


FIG. 1. (a), (b) Differential resistance of a nanopillar spin valve device as a function of magnetic field and (c), (d) as a function of current, measured at (a), (c)  $T = 295$  K and (b), (d)  $T = 4.2$  K.

microwave measurements [10] on similar samples, we have identified this increase as due to the excitation of dynamical states ( $D$ ) in which the free layer undergoes steady-state precessional motion.

Based on 4.2 K measurements of  $dV/dI$  as a function of  $I$  at a fixed  $H$  and as a function of  $H$  at a fixed  $I$ , we construct the phase diagram shown in Fig. 2(a), indicating at what values of  $H$  and  $I$  the different static and dynamic states are stable or bistable. This phase diagram is in good agreement with numerical [10] and analytical [19] solutions of the LLG equations. The phase diagram is shifted along the  $H$  axis due to  $H_d$ , which allows us to access the regime where the total field ( $H - H_d$ ) acting on the free layer is opposite to the fixed layer moment and thus to the current polarization.

Throughout the temperature range between 4.2 K and 300 K,  $I$  and  $H$  can be adjusted to bias points at which the sample resistance exhibits two-level fluctuations as a function of time, corresponding to transitions of the Py free layer between high (HR) and low (LR) resistance states [e.g., Fig. 2(b), inset]. The bias conditions for which the dwell times in both HR and LR states are  $\sim 1$  ms are plotted in Fig. 2(a) for 16 values of  $T$ . In Fig. 2(b), we show the difference in dc resistance between the HR ( $R_H$ ) and the LR ( $R_L$ ) states of the telegraph signal, normalized by the full resistance difference ( $R_{AP} - R_P$ ) between the

AP and P states for  $I = 0$  at the measurement temperature. We find that switching between the fully P and AP states occurs only for currents between  $-0.2$  mA and  $0.4$  mA [Fig. 2(b)]. The smaller changes in  $R$  elsewhere indicate that for  $I < -0.2$  mA the telegraph signals correspond to transitions between the P state and the dynamical state ( $D$ ) with intermediate resistance, and for  $I > 0.4$  mA the transitions are between the AP and  $D$  states. These identifications are consistent with the positions of the bistable modes in the 4.2 K phase diagram [Fig. 2(a)] and with the predicted phase diagram [19].

Before we discuss how the measured switching rates depend on  $I$ ,  $H$ , and  $T$ , we will review the competing predictions. In general, the dwell time of a thermally activated switching process can be parameterized in the form

$$\tau = \tau_0 \exp\left(\frac{E_a(H, I)}{k_B T^*}\right), \quad (1)$$

where  $\tau_0$  is an attempt time,  $T^*$  is an effective temperature,  $E_a(H, I)$  is an effective activation barrier, and  $k_B$  is the Boltzmann constant. Within the model of coherent spin-transfer torques, analyzed in the framework of the LLG equation [12,17,20,21],  $T^*$  is simply the true sample temperature,  $T$ . Even though the spin-transfer torques are nonconservative, an argument based on the fluctuation-dissipation theorem predicts that the effect of  $I$  in this model for a uniaxial magnet undergoing P-AP switching can nevertheless be understood as a linear change in  $E_a$ ,  $E_a(I) \propto 1 - I/I_C$  [20,22]. The same functional form has also been found for the more general case both analytically and from numerical solutions of the LLG equation [17,21]. In contrast, quite different predictions are given by the model in which a spin-polarized current excites incoherent short-wavelength magnons and affects magnetic reversal by raising the effective temperature  $T^*(I)$  of the free layer. Since spin-flip scattering is only enhanced when the current polarization is opposite to the moment of the free layer, this model predicts an increased  $T^*(I)$  only for the P state (for  $I > 0$ ) or the AP state (for  $I < 0$ ), but not for both states simultaneously. The degree of heating has been argued to be very large and to increase with increasing  $|I|$ , e.g. 400 K/mA above a threshold current for devices in ref. [13], and 500 K to 1100 K in ref. [14]. In the magnetic heating model,  $E_a(H, I)$  should depend only weakly on the  $I$  through a decrease of the magnet's moment with increasing  $T^*(I)$ .

In Fig. 3 we show measured average  $\tau$  for the HR and LR states of the telegraph signal for  $I < 0$  (a,c) and  $I > 0$  (b,d), plotted logarithmically as a function of  $1/T$ . Figs. 3(a) and 3(b) correspond to high  $T$  (200–300 K), in the range of  $I$  where transitions are between P and AP states, while Figs. 3(c) and 3(d) correspond to low  $T$  (4.2–25 K) for switching between P and  $D$  states and between  $D$  and AP states. For each set of data corresponding to a given value of  $I$ , we first tune  $H$  so that  $\tau$  in the

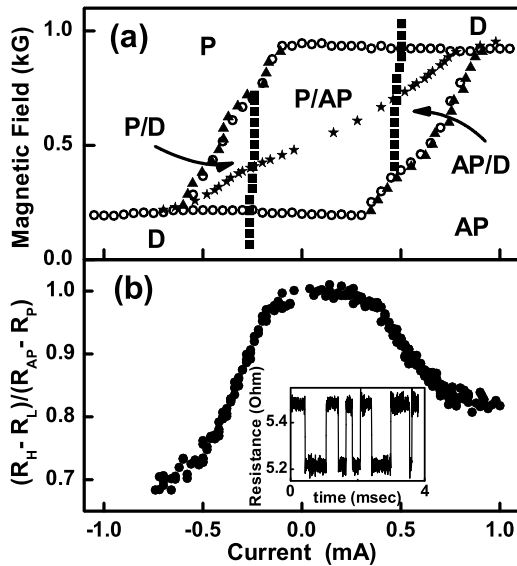


FIG. 2. (a) Phase diagram of magnetic states for the Py free layer at  $T = 4.2$  K obtained from measurements of  $dV/dI$  as a function of  $I$  at fixed  $H$  ( $\blacksquare$ ,  $I_D^\pm$ ;  $\blacktriangle$ ,  $I_S^\pm$ ) and as a function of  $H$  at fixed  $I$  ( $\circ$ ). Stars ( $\star$ ) mark  $I$  and  $H$  values for which the dwell times in both the HR and LR states are approximately equal to 1 ms, at 16 temperatures ranging from 300 K at small  $|I|$  to 4.2 K at large  $|I|$ . (b) The current dependence of the amplitude of two-level resistance fluctuations, normalized by the full difference in resistance between the P and AP states of the nanopillar. Inset: Two-level fluctuations between the HR and LR states for  $I = 1.0$  mA,  $H = 956.6$  G,  $T = 4.2$  K.

two states are approximately equal, and then vary  $T$  at fixed  $I$  and  $H$ . Several conclusions can be drawn from these data. First, for all transitions at  $T \geq 20$  K,  $\ln(\tau)$  depends linearly on  $1/T$ , so that the transitions are thermally activated. As  $H$  and  $I$  are varied, the slopes of the lines change, meaning that the transitions remain thermally activated but  $E_a$  is modified. At low  $T$  and large  $I$ , the  $D \rightarrow P$  and  $P \rightarrow D$  dwell times [Fig. 3(c)] display an almost identical dependence on  $T$ , remaining approximately equal even as they both vary by several orders of magnitude. Similar behavior is seen for  $D \rightarrow AP$  and  $AP \rightarrow D$  transitions [Fig. 3(d)] and the  $P \rightarrow AP$  and  $AP \rightarrow P$  transitions [Fig. 3(a)]. This shows, in contrast to the magnetic heating model, that the free layer is not heated to a high effective temperature that depends on the orientation of its moment relative to the direction of the current polarization. The different slopes for  $P \rightarrow AP$  and  $AP \rightarrow P$  transitions in Fig. 3(b) are not due to heating, but to different sensitivities to  $T$ -dependent magnetic parameters [see Eq. (3) and discussion below].

While the dwell times for transitions between static and dynamical states in Figs. 3(c) and 3(d) exhibit thermal-activation behavior linear in  $1/T$  for  $T \geq 20$  K, they saturate below  $\sim 10$  K. We conclude that heating

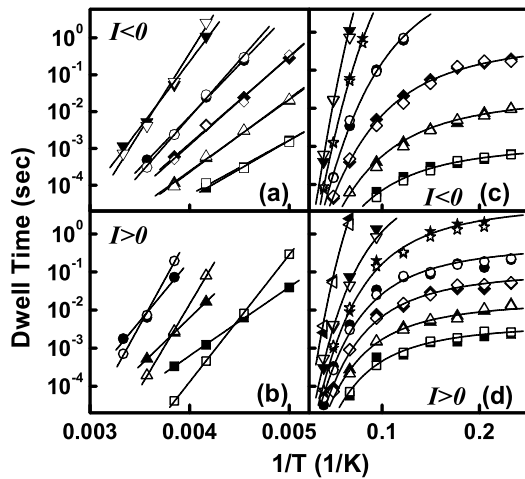


FIG. 3. Temperature dependence of dwell times for the two-level resistance fluctuations measured at fixed  $I$  and  $H$ . (a)  $AP \rightarrow P$  (open symbols) and  $P \rightarrow AP$  (solid symbols) dwell times: ( $\square, \blacksquare$ )  $-0.26$  mA,  $400.8$  G; ( $\triangle, \blacktriangle$ )  $-0.22$  mA,  $415.3$  G; ( $\diamond, \blacklozenge$ )  $-0.18$  mA,  $430.7$  G; ( $\circ, \bullet$ )  $-0.14$  mA,  $446.4$  G; ( $\nabla, \blacktriangledown$ )  $-0.04$  mA,  $482.8$  G. (b)  $AP \rightarrow P$  (open symbols) and  $P \rightarrow AP$  (solid symbols) dwell times: ( $\square, \blacksquare$ )  $0.46$  mA,  $709.2$  G; ( $\triangle, \blacktriangle$ )  $0.36$  mA,  $649.4$  G; ( $\circ, \bullet$ )  $0.16$  mA,  $561.6$  G. (c)  $P \rightarrow D$  (open symbols) and  $D \rightarrow P$  transitions (solid symbols) dwell times: ( $\square, \blacksquare$ )  $-0.72$  mA,  $213.1$  G; ( $\triangle, \blacktriangle$ )  $-0.70$  mA,  $217.8$  G; ( $\diamond, \blacklozenge$ )  $-0.68$  mA,  $222.6$  G; ( $\circ, \bullet$ )  $-0.66$  mA,  $226.8$  G; ( $\star, \blackstar$ )  $-0.64$  mA,  $230.9$  G; ( $\nabla, \blacktriangledown$ )  $-0.62$  mA,  $235.7$  G. (d)  $D \rightarrow AP$  (open symbols) and  $AP \rightarrow D$  (solid symbols) dwell times: ( $\square, \blacksquare$ )  $0.98$  mA,  $953.5$  G; ( $\triangle, \blacktriangle$ )  $0.96$  mA,  $950.7$  G; ( $\diamond, \blacklozenge$ )  $0.94$  mA,  $947.5$  G; ( $\circ, \bullet$ )  $0.92$  mA,  $944.7$  G; ( $\star, \blackstar$ )  $0.90$  mA,  $941.3$  G; ( $\nabla, \blacktriangledown$ )  $0.88$  mA,  $936.9$  G; ( $\triangleleft, \blacktriangleleft$ )  $0.84$  mA,  $928.2$  G. The lines are fits using Eqs. (1)–(3).

by the current becomes non-negligible in this regime. However, this degree of heating is expected simply from ohmic dissipation in a diffusive metal wire, without more complicated considerations involving magnetic excitations. If heat flow from the device is dominated by electronic conduction to the contacts rather than by phonon mechanisms, the maximum electronic temperature  $T_{el}$  in a metal wire is

$$T_{el} = \sqrt{T^2 + \frac{3}{4} \left( \frac{eIR}{\pi k_B} \right)^2}, \quad (2)$$

where  $e$  is the electron charge [23]. The lines in Figs. 3(c) and 3(d) are fits to the data using Eq. (1), with  $T^* = T_{el}$  and with  $E_a(H, I)$  and  $\tau_0$  as fitting parameters. The quality of the fits supports the picture of ohmic heating. For our highest currents at  $4.2$  K, the largest  $T_{el}$  that we measure is less than  $20$  K.

From linear fits to the high  $T$  data [Fig. 3(a) and 3(b)], one may attempt to determine  $E_a(H, I)$  and  $\tau_0$ . However, this process can yield unphysical results (e.g.  $\tau_0 < 10^{-17}$  s), because the slopes of the  $\ln(\tau)$  versus  $1/T$ , and hence  $E_a$ , are affected by the  $T$ -dependence of the sample's magnetic parameters, particularly in the high  $T$  range. In order to obtain quantitative results for  $E_a$ , we have therefore analyzed the dwell times in a way that takes into account these  $T$ -dependences. We find that the evolution of  $E_a$  is consistent with the assumption that its dependence on  $H$  and  $I$  factors [20,21], in the form

$$E_S(H, I) = \varepsilon_S(I) \frac{H_K(T)m(T)}{2} \left( 1 \pm \frac{H - H_d(T)}{H_K(T)} \right)^{3/2}, \quad (3)$$

where  $S = HR$  or  $LR$  labels the activation barrier for transitions out of the  $HR$  or  $LR$  states,  $H_K(T)$  is the shape anisotropy field of the free layer, and  $m(T)$  is the magnetic moment of the free layer. The plus (minus) sign corresponds to the  $LR \rightarrow HR$  ( $HR \rightarrow LR$ ) transition. The functions  $\varepsilon_S(I)$  characterize the current dependence of the activation energies; they satisfy a normalization condition  $\varepsilon_S(0) = 1$  so that we recover the Néel-Brown activation barrier for  $I = 0$  [24]. To determine the required  $T$ -dependences, we assume that both  $m(T)$  and  $H_K(T)$  are proportional to magnetization ( $M$ ) of the Py free layer. We use SQUID magnetometry to measure  $M(T)$  for a  $2$  nm Py film in a Cu/Py/Cu trilayer that is exposed to the same heat treatments used during fabrication of the nanopillars [25]. The value of  $H_K = 375$  G at  $4.2$  K is determined from the half-width of the hysteresis loop [Fig. 1(b)] and the value of  $m$  at  $4.2$  K is determined from  $\varepsilon_S(0) = 1$ . We can measure  $H_d$  directly for our device from variations of the hysteresis loop shift with  $T$  [e.g., Fig. 1(a) and 1(b)]. We find a  $19\%$  decrease of  $M$  from  $20$  K to  $300$  K [25] while  $H_d$  decreases by  $14\%$  from  $4.2$  K to  $295$  K. The lines in Fig. 3(a) and 3(b) are fits to the data using Eqs. (1)–(3) with  $\varepsilon_S(I)$  and  $\tau_0$  as fitting parameters, yielding a physically reasonable  $\tau_0 = 10^{-9.0 \pm 1.5}$  s. The different slopes for the two dwell times in Fig. 3(a) and

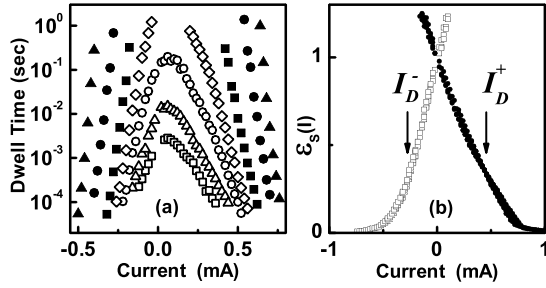


FIG. 4. (a) Measured dwell times as a function of  $I$  at the field  $H_{eq}(I, T)$  for which the average dwell times for LR  $\rightarrow$  HR and HR  $\rightarrow$  LR transitions are equal, for the temperatures  $\square$  300 K,  $\triangle$  280 K,  $\circ$  260 K,  $\diamond$  240 K,  $\blacksquare$  200 K,  $\bullet$  140 K, and  $\blacktriangle$  80 K. (b) The activation barriers  $\square$   $\varepsilon_{HR}(I)$  for switching HR  $\rightarrow$  LR and  $\bullet$   $\varepsilon_{LR}(I)$  for switching LR  $\rightarrow$  HR, obtained by using Eq. (4) to collapse data such as in (a) for 16 temperatures between 4.2 and 300 K.

3(b) originate from the  $T$ -dependence of  $|H - H_d|/H_K$  as described by Eq. (3). This parameter is a stronger function of  $T$  for  $H - H_d > 0$ , since  $|H - H_d|$  increases and  $H_K$  decreases with  $T$  [Fig. 3(b)], and a weaker function of  $T$  for  $H - H_d < 0$ , since both  $|H - H_d|$  and  $H_K$  decrease with  $T$  [Fig. 3(a)].

By combining Eqs. (1)–(3), and assuming that  $\tau_0$  in the HR and LR states are approximately equal, we arrive at a simple expression for  $\varepsilon_S(I)$  [26]:

$$\varepsilon_S(I) = \frac{2k_B T_{el} [\ln(\tau_S) - \ln(\tau_0)]}{H_K(T) m(T) (1 \pm \frac{H - H_d(T)}{H_K(T)})^{3/2}}. \quad (4)$$

We can use Eq. (4) to rescale  $\tau_S$  measured at different values of  $H$ ,  $I$ , and  $T$  [Fig. 4(a)], onto common curves for  $\varepsilon_{HR}(I)$  and  $\varepsilon_{LR}(I)$  [Fig. 4(b)]. The only unknown parameter in the analysis is  $\tau_0$ . A value of  $\tau_0 = 10^{-9}$  s gives the best collapse of data sets at 16 different temperatures onto just two curves for  $\varepsilon_{HR}(I)$  and  $\varepsilon_{LR}(I)$ . The high quality of the data collapse in Fig. 4(b) provides justification for the form of the  $I$ -dependence asserted in Eq. (3), and it shows that the effect of a spin-polarized current on magnetic switching can be described accurately in terms of  $I$ -dependent activation barriers for the magnetic states. In the range of  $I$  where transitions occur between static P and AP states, the activation barriers depend linearly on  $I$  as predicted by models of coherent spin-transfer torques that use the LLG equation [20,21]. However, at  $|I| > I_D$ , for transitions from the dynamical to static states, the activation barriers appear to be weaker functions of  $I$ .

The value of  $m$  at 4.2 K determined by our analysis is  $m = (5.1 \pm 0.8) \times 10^{-15}$  emu. This can be compared to the expected value  $m = MV = 7.9 \times 10^{-15}$  emu, where  $M = 645$  emu/cm<sup>3</sup> at 20 K [25] and  $V = 1.23 \times 10^{-17}$  cm<sup>3</sup> is the estimated volume of the nanomagnet based on electron microscopy. We conclude that the activation volume of the free layer for thermally assisted reversal is close to its physical volume and thus the nano-

magnet behaves as a Néel-Brown nanoparticle [27] from 4.2 K to 300 K.

In conclusion, we have performed measurements of magnetic switching rates for a nanomagnet under the influence of a spin-polarized current. The data are in good agreement with the spin-torque model, in which spin-transfer causes a coherent rotation of the local magnetic moment that can be modeled by the LLG equation. The data are not consistent with arguments that incoherent magnon generation can drive a nanomagnet to effective temperatures well above room temperature. The overall effect of the current on magnetic switching is well described in terms of current-dependent activation barriers.

We acknowledge support from DARPA through Motorola, from the Army Research Office, and from the NSF/NSEC program through the Cornell Center for Nanoscale Systems. We also acknowledge NSF support through use of the Cornell Nanofabrication Facility/NNIN and the Cornell Center for Materials Research facilities.

- 
- [1] J. C. Slonczewski, *J. Magn. Magn. Mater.* **159**, L1 (1996).
  - [2] L. Berger, *Phys. Rev. B* **54**, 9353 (1996).
  - [3] M. Tsoi *et al.*, *Phys. Rev. Lett.* **80**, 4281 (1998).
  - [4] E. B. Myers *et al.*, *Science* **285**, 867 (1999).
  - [5] J. A. Katine *et al.*, *Phys. Rev. Lett.* **84**, 3149 (2000).
  - [6] J.-E. Wegrowe *et al.*, *Europhys. Lett.* **45**, 626 (1999).
  - [7] J. Z. Sun, *J. Magn. Magn. Mater.* **202**, 157 (1999).
  - [8] J. Grollier *et al.*, *Appl. Phys. Lett.* **78**, 3663 (2001).
  - [9] F. J. Albert *et al.*, *Appl. Phys. Lett.* **77**, 1357 (2000).
  - [10] S. I. Kiselev *et al.*, *Nature (London)* **425**, 380 (2003).
  - [11] W. H. Rippard *et al.*, *Phys. Rev. Lett.* **92**, 027201, (2004).
  - [12] E. B. Myers *et al.*, *Phys. Rev. Lett.* **89**, 196801 (2002).
  - [13] S. Urzhudin *et al.*, *Phys. Rev. Lett.* **91**, 146803 (2003).
  - [14] A. Fábian *et al.*, *Phys. Rev. Lett.* **91**, 257209 (2003).
  - [15] M. D. Stiles and A. Zangwill, *Phys. Rev. B* **66**, 014407 (2002).
  - [16] J. Z. Sun, *Phys. Rev. B* **62**, 570 (2000).
  - [17] Z. Li and S. Zhang, *Phys. Rev. B* **68**, 024404 (2003).
  - [18] F. J. Albert *et al.*, *Phys. Rev. Lett.* **89**, 226802 (2002).
  - [19] T. Valet, report.
  - [20] R. H. Koch, J. A. Katine, and J. Z. Sun, *Phys. Rev. Lett.* **92**, 088302 (2004).
  - [21] Z. Li and S. Zhang, *Phys. Rev. B* **69**, 134416 (2004).
  - [22] This effective activation barrier is equivalent to a fictitious temperature  $T/(1 - I/I_C)$ , proportional to  $T$  [20].
  - [23] R. Holm, *Electric Contacts* (Springer-Verlag, Berlin, 1967), p. 63.
  - [24] R. H. Victora, *Phys. Rev. Lett.* **63**, 457 (1989).
  - [25] For the 2 nm Py layer we measure  $M = 645$  emu/cm<sup>3</sup> at 20 K, reduced from 880 emu/cm<sup>3</sup> for bulk Py, and a stronger  $T$  dependence.
  - [26] In principle,  $\varepsilon_S(I)$  may also depend on  $H$ . However, our determination of  $\varepsilon$  is not sensitive to  $I$  and  $H$  independently, since data were taken at  $\tau_{HR} \approx \tau_{LR}$ , along one line in the  $(H, I)$  plane.
  - [27] W. Wernsdorfer *et al.*, *Phys. Rev. Lett.* **78**, 1791 (1997).